Time-gated Single Photon Counting Lock-in Detection at 1550 nm Wavelength

Liantuan Xiao, Xiaobo Wang, Guofeng Zhang and Suotang Jia
State Key Laboratory of Quantum Optics and Quantum Optics Devices,
College of Physics and Electronics Engineering, Shanxi University,
Taiyuan 030006,
China

1. Introduction

Time-gated single photon counting (TGSPC), which employs a single photon detector as the detection apparatus (Poultney, 1972; 1977), has received increasing attention because of its superior spatial resolution and the absence of the so-called classical dead zones (Forrester & Hulme, 1981). TGSPC is a repetitively pulsed statistical sampling technique that records the time of arrival of photons and logs this against the time of emission of a laser pulse. TGSPC have become increasingly important in a number of applications such as time-resolved photoluminescence (Dixon, 1997; Leskovar & Lo, 1976), optical time-domain reflectometry (Lacaita et al., 1993; Benaron & Stevenson, 1993; Wegmüller et al., 2004), time-of-flight laser ranging (Pellegrini et al., 2000; Carmer & Peterson, 1996) and 3D imaging (Moring et al., 1989; Mäkynen et al., 1994).

Ultrasensitive detection with single photon detection capability requires detectors high quantum efficiency and low dark noise. Operation in the 1550 nm spectral region enables it to be worked in fiber, and the eye-safe ranging brings it to be carried out in daylight conditions. In the 1550 nm wavelength implementations, InGaAs/InP avalanche photodiode detectors (APDs) are commonly used (Pellegrini, et al., 2006; Hiskett, et al., 2000; Lacaita, et al., 1996). However, these APDs have low quantum efficiency because the photons may pass through the very thin depletion layer without being absorbed. In addition, these single-photon detectors exhibit high afterpulse probability, which can cause significant distortion for the measurements. In order to reduce this effect these detectors have to be operated in a time-gated mode. As each photon's arrival time is an independent measure of range, and accuracy can be improved by increasing the number of samples. Unfortunately, direct photon counting will induce the quantum fluctuation (i.e. shot noise).

Time-correlated single-photon counting (TCSPC) is a repetitively pulsed statistical sampling technique that records the time of arrival of photons reflected from a target and logs this against the time of emission of a laser pulse (Becker, 2005). Each photon's arrival time is an independent measure of flight, and accuracy can be improved by increasing the number of samples. However, the technique's main disadvantage is an extended data-acquisition time being required where the illumination noise is a serious problem.

Weak light detection can be improved by use of the lock-in principle (Stanford Research Systems, 1999). A lock-in detects a signal at a known modulation frequency in amplitude

and phase and suppresses noise at other frequencies. The lock-in detection principle can enhance the signal-to-noise ratio (SNR) by orders of magnitude. The lock-in principle was first applied to photon-counting detection by Arecchi *et al. (*Arecchi et al. 1966*)* and was used subsequently in many low-light measurements (Murphy et al., 1973; Alfonso & Ockman, 1968). A dual-phase implementation of the gated photon counting is hampered by signal pick up from harmonics under nonsinusoidal modulation (Stanford Research Systems, 1995). To obtain a precise phase signal, photon counts were reconverted to analog signals that feed into a lock-in amplifier (Braun & Libchaber, 2002). In a previous publication we have demonstrated that the wavelength modulation lock-in can improve the SNR of photon counting for weak fluorescence effectively and eliminate the quantum fluctuation (Huang et al., 2006).

In this chapter, we present an overview of the principle of single-photon detection at 1550nm. And then we focus on the question of illumination noise, detector dark count noise and the detection efficiency of single-photon detector, and we show that the novel method of photon-counting lock-in for TGSPC detection can suppress background noise, and importantly, enhance the detection efficiency of single photon detector.

2. Single photon detection at 1550nm

2.1 Single photon avalanche diodes

An avalanche photodiode reverse-biased above its breakdown voltage, V_{bd}, allows single photon detection (Ribordy et al., 1998). When such a diode is biased above V_{bd}, it remains in a zero current state for a relatively long period of time, usually in the millisecond range. During this time, a very high electric field exists within the p-n junction forming the avalanche multiplication region.

Under these conditions, if a primary carrier enters the multiplication region and triggers an avalanche process, several hundreds of thousands of secondary electron-hole pairs are generated by impact ionization, thus causing the diode's depletion capacitance to be rapidly discharged (Stucki, 2001). As a result, a sharp current pulse is generated and can be easily measured. This mode of operation is commonly known as Geiger mode (Ribordy et al., 2004). Unfortunately, typical photodiodes, as those used in conventional imagers, are not compatible with this mode of operation since they suffer from a premature breakdown when the bias voltage approaches V_{bd}. Premature breakdown occurs since the peak electric field is located only in the diode's periphery rather than in the planar region. A single photon avalanche diode (SPAD), on the other hand, is a specifically designed photodiode in which premature breakdown is avoided and a planar multiplication region is formed within the whole junction area (Hadfield, 2009).

Linear mode avalanche photodiodes, which are biased just below V_{bd}, have a finite multiplication gain. Statistical variations of this finite gain produce an additional noise contribution known as excess noise (Tilleman & Krishnaswami, 1996; Yano et al., 1990). SPADs, on the other hand, are not concerned with these gain fluctuations since the optical gain is virtually infinite (Takesue et al., 2006). Nevertheless, the statistical nature of the avalanche buildup is translated onto a detection probability. Indeed, the probability of detecting a photon hitting the SPAD's surface depends on the diode's quantum efficiency and the probability for an electron or for a hole to trigger an avalanche (Legre et al., 2007). Intensity information is obtained by counting the pulses during a certain period of time or by measuring the mean time interval between successive pulses. The same mechanism may

be used to evaluate noise. Thermally or tunneling generated carriers within the p-n junction, which produce dark current in linear mode photodiodes, can trigger avalanche pulses. In Geiger mode, they are indistinguishable from regular photon-triggered pulses and they produce spurious pulses at a frequency known as *dark count rate* (DCR). DCR strongly depends on temperature and it is an important parameter for a TGSPC since it generates false measurements (Thew et al., 2007).

The practical detection efficiency, η, is defined as the overall probability of registering a count if a photon arrives at the detector. In most photon-counting applications a high value of η is certainly desirable. The higher the value of η, the smaller the signal loss, thus results more efficient and accurate measurements. DCR and detection efficiency determine the lowest power that is detectable by the device through the noise equivalent power (NEP) which is defined as $NEP = h\nu\sqrt{2D}/\eta$, here $h\nu$ is the energy of the signal photon, and D is the DCR (Hiskett, 2001; Gisin et al., 2002).

Another source of spurious counts is represented by *after-pulses* (Roussev et al., 2004). They are due to carriers temporarily trapped after a Geiger pulse in the multiplication region that are released after a short time interval, thus re-triggering a Geiger event. After-pulses depend on the trap concentration as well as on the number of carriers generated during a Geiger pulse. The number of carriers depends in turn on the diode's parasitic capacitance and on the external circuit, which is usually the circuit used to quench the avalanche. Typically, the quenching process is achieved by temporarily lowering the bias voltage below V_{bd}. Once the avalanche has been quenched, the SPAD needs to be recharged again above V_{bd} so that it can detect subsequent photons. The time required to quench the avalanche and recharge the diode up to 90% of its nominal excess bias is defined as the *dead time*. This parameter limits the maximal rate of detected photons, thus producing a saturation effect (Dixon, et al., 2008).

The commercially available InGaAs/InP avalanche photodiode has been the most practical device for SPADs at 1550nm telecommunication wavelength (Warburton et al., 2009). Since a photo-excited carrier grows into a macroscopic current output via the carrier avalanche multiplication in an APD operated in the Geiger mode, a single-photon can be detected efficiently. However, fractions of the many carriers trapped in the APD are subsequently emitted, and trigger additional avalanches that cause erroneous events. The InGaAs/InP SAPD in Geiger mode has a particularly high probability that afterpulses occur. Therefore, the InGaAs/InP SAPD is usually operated in the gated mode in which the gate duration (gate-on time) is generally set to a few nanoseconds (Namekata et al., 2006; Yoshizawa et al., 2004). Then the interval between two consecutive gates is set to more than the lifetime (in orders of microseconds) of the trapped carriers so that the afterpulse is suppressed. As a result, the repetition frequency of the gate has been limited to several megahertz, which is unsuitable for applications such as the high-speed detection (Hadfield et al., 2006).

2.2 The block diagram for single photon detector at 1550nm

Fig. 1 shows a typical block diagram scheme for a commercially single photon detector, Photon Counting Receiver PGA 600 manufactured by Princeton Lightwave Inc (Princeton Light Wave, 2006). The receiver has four major functional elements. These are the InGaAs SPAD, analog signal processing circuitry, a discriminator circuitry, and triggering, biasing and blanking circuitry.
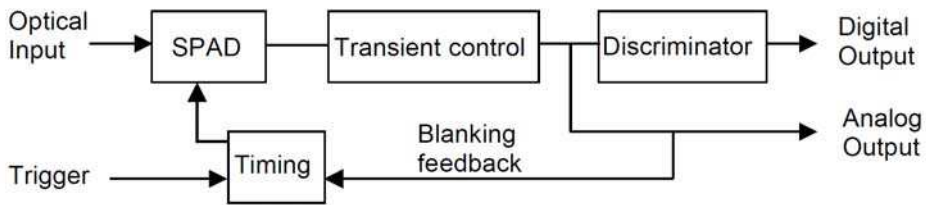
Fig. 1. The typical block diagram scheme for 1550nm single photon detector.

The SAPD is operated at ~ 218 K to reduce the probability of DCR. When the detector is triggered, the APD bias voltage is raised above its reverse V_{bd} to operate in Geiger mode. A short time later the bias is reduced below V_{bd} again to prevent false events.

The analog signal processing circuitry eliminates the transient noise created when a short bias pulse is applied to the SPAD, and isolates the charge pulse that results when a photon trigger an avalanche event.

The discriminator circuitry generates a digital logic pulse when the pulse-height of an analog charge signal exceeds a threshold level set to reject electronic noise. In a typical photon counting system, the SPAD output exhibits fluctuations in the pulse height and these pulses are amplified and directed into the discriminator. The discriminator compares the input pulses with the preset reference threshold voltage, where the lower pulses are eliminated. The higher pulses output at a constant level, usually as transistor-transistor logic (TTL) level from 0V to 5 V, allowing counting the discriminated pulses. To increase the detection efficiency, it is advantageous to set the level discrimination at a lower position, but this is also accompanied by a noise increase thus increasing dark count and the NEP.

The triggering circuitry initiates bias pulse generation when a trigger pulse reaches a set threshold level.

The delay between triggering and bias pulse generation can be adjusted so that the bias pulses accurately coincide with the expected arrival times of the photons. By using short bias pulses, the probability of dark counts can be significantly reduced, improving the detector's SNR performance.

When the detector is triggered, the SPAD bias voltage is raised above its reverse breakdown voltage to operate in Geiger mode. This feature is useful to suppress afterpulsing of the SPAD. The detector has both of digital and analog output. The discriminator circuitry generates a digital logic pulse when the pulse-height of an analog charge signal exceeds a threshold level set to reject electronic noise. The threshold is set as the cross-over voltage at which background noise and the single photon make equal contributions to the pulse height distribution. With the certain threshold, the receiver provides 20% detection efficiency and 10^{-5} dark count probability per 1 ns gating pulse.

2.3 Quantum fluctuations and SNR of photon counting

The SPAD records the incident photons in the sampling time τ. Suppose the average photon count is a, the quantum fluctuations of the photon counting distribution can be expressed as (Lee et al., 2006)

$$I_{sn} = \sqrt{\sum_n P(n)(n-\alpha)^2} \ , \tag{1}$$

where n is the actual photon numbers measured during the experiment.

For the coherent light field, the photon counting distribution obeys Poisson distribution

$$P_c(n) = \alpha^n e^{-\alpha} / n! \, . \tag{2}$$

The quantum fluctuations of coherent light field should be

$$I_{sn}^c = \sqrt{\alpha} \, . \tag{3}$$

The SNR of photon counting can be expressed as

$$SNR = \frac{\alpha \tau}{\sqrt{(\alpha + B + D)}} = \frac{\alpha}{\sqrt{(\alpha + B + D)}} \sqrt{\tau} \, . \tag{4}$$

Where B is the photon count rate caused by illumination noise light. When the background stray light and the dark counts of detector, working in low-temperature environment, can be ignored compared to signal counts, the maximum value $(\alpha \tau)^{1/2}$ of spectral SNR can be obtained. Increasing τ could get a higher SNR, but the temporal resolution should be decreased in this way.

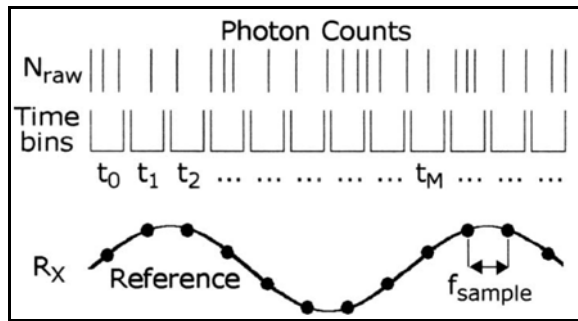## 2.4 The principle of photon counting lock-in

Fig. 2. Implementation of the photon-counting lock-in.

Lock-in amplifier is a synchronous coherent detector using principle of cross-correlation, extracting useful signals from noise because the reference signal frequency related to the input signal frequency but not related to noise frequency. It is equivalent to a very narrow bandwidth band-pass filter, and it is necessary to compress the filter bandwidth as much as possible in order to suppress noise.

When the incident photons were intensity modulated by the sine-wave of frequency f_s, the instantaneous photon counts at time t is expressed as $r_0 + m\cos(2\pi f_s t)$, where r_0 is average photon counts, m is depth of modulation. Then within the sampling time τ the effective photon counts can be expressed as (Huang et al., 2006)

$$r_t(\tau) = r_0 + m\left[\frac{\sin(\pi f_s \tau)}{\pi f_s \tau}\right]\cos(2\pi f_s t + \pi f_s \tau) \, . \tag{5}$$

The probability of n photon being detected in the sampling time τ is

$$p(n) = \frac{e^{-r_t(\tau)}(r_t(\tau))^n}{n!} .$$ (6)

As shown in Fig. 2, projections of time-binned photon counts N_{raw} to sinusoidal reference R_X are time averaged to yield the small I_X signal of the lock-in.

The photon counts lock-in needs the signal to be converted to analog signal to fulfill the input demand of lock-in amplifier, where only the frequency components corresponding with the demodulation filter bandwidth will be retained. Reduction of noise imposed upon a useful signal with frequency f_s, is proportional to the square root of the bandwidth of a bandpass filter Δf, centre frequency f_s.

The SNR of demodulated signal is

$$SNR = \frac{S_N}{(I_{sn} + I_{ex})(\Delta f / f_n)} .$$ (7)

Where S_N is the analog signal of the photon counts, I_{ex} is excess noise. f_n is the noise distribution bandwidth of need to be measured signal. Compressing the filter bandwidth Δf makes the corresponding noise signal decreases, as a result enhance the SNR of TGSPC measurement.

3. Photon-counting lock-in for TGSPC detection

3.1 Experiment setup

The diagram of the photon counting lock-in for TGSPC measurement is as shown in Fig. 3. A 1550nm wavelength, 300-ps pulse length laser (id300, ID Quantique), external triggered
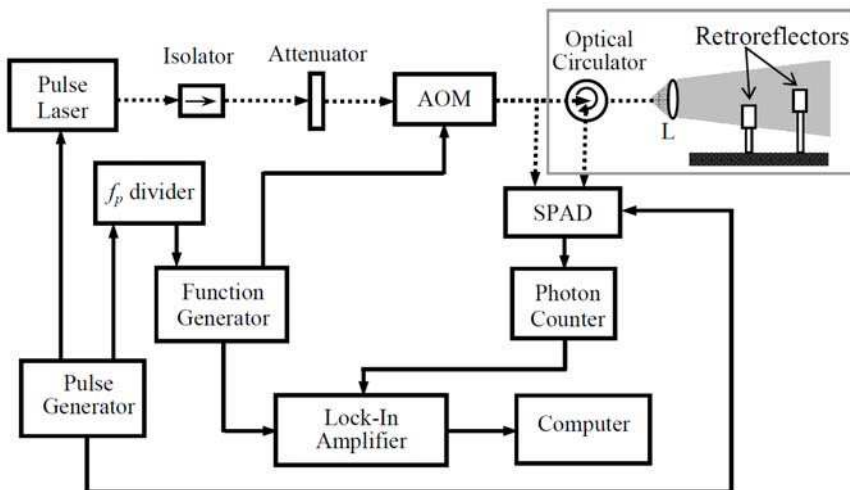

Fig. 3. Schematic diagram of photon counting lock-in experiment. AOM is acousto-optic modulator. SPAD is Photon Counting Benchtop Receiver with an InGaAs single photon detector. The dashed line range is the setup for TGSPC measurement.

by a pulse generator (SRS DG645) at f_p=4MHz repetition rate, is attenuated to produce a suitable (~5–100kcps) counting rate in the detector. The weak laser pulses were intensity modulated with a frequency-downshifted (200MHz) acousto-optic modulator (AOM, M200-2J-F2S Gooch & Housego). A sine-wave function generator is triggered by the variable divider from laser pulses frequency, worked as the modulation signal and added onto the AOM's driver. The weak pulses are launched into the PCBR and incidence on the SPAD. Meanwhile, the synchronizing TTL pulses from DG535 were used to trigger the SPD. The analog output of the SPD is connected to the photon counter (SRS SR400); and the photon counting signal is demodulated by the lock-in amplifier (SRS SR830). The experiment control and the data collection were completed by Labview software.

Two identical air-filled retroreflecting corner cubes were attached to translation stages and mounted on an optomechanical rail that was positioned at a range of approximately 10 m from the fiber coupler lens. The optics of the laser diode was configured so that both corner cubes were illuminated, and the photon returns were collected by the same lens.
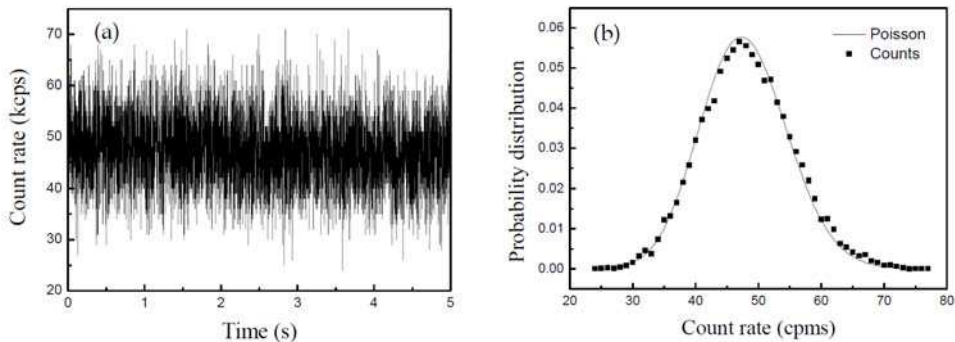

Fig. 4. Quantum fluctuation of photons counting (a) and its statistics characteristics (b).

3.2 Photon counts lock-in results

The photon counts were converted to analog signal by using SR400 with the digital-analog conversion factor g=0.1mV/count. A sine-wave signal, with repetition frequency f_s=10Hz, peak-to-peak voltage V_{pp}=300mV and offset voltage V_{off}=370mV, worked as the modulation signal and was added onto the AOM's driver.

The directly photon counting TGSPC measurement is shown in Fig. 4 (a), the average photon number is a=50kcps, sampling time τ=1ms. It is found of the quantum fluctuations of photon counting obviously. The data points in Fig.4 (b) are statistical characteristics of photon counting in Fig.4 (a). The solid line is fitted curve of Poisson distribution function. As can be seen from the figure, the photon counting of coherent light field obeys Poisson distribution.

Fig. 5 (a) is an analog signal of the photon counts after the digital-analog converted in photon counting TGSPC of the retroreflector. Fig. 5 (b) is the Fourier transforms (FFT) results of analog signal in Fig. 5 (a). We found that the noise amplitude distribution of the photon counting quantum fluctuations is a uniform distribution in the frequency domain. Lock-in method here will not be affected by the low frequency $1/f$ noise. The magnitude of carrier signal is about -8dB at the location of 10Hz modulation frequency, two orders of
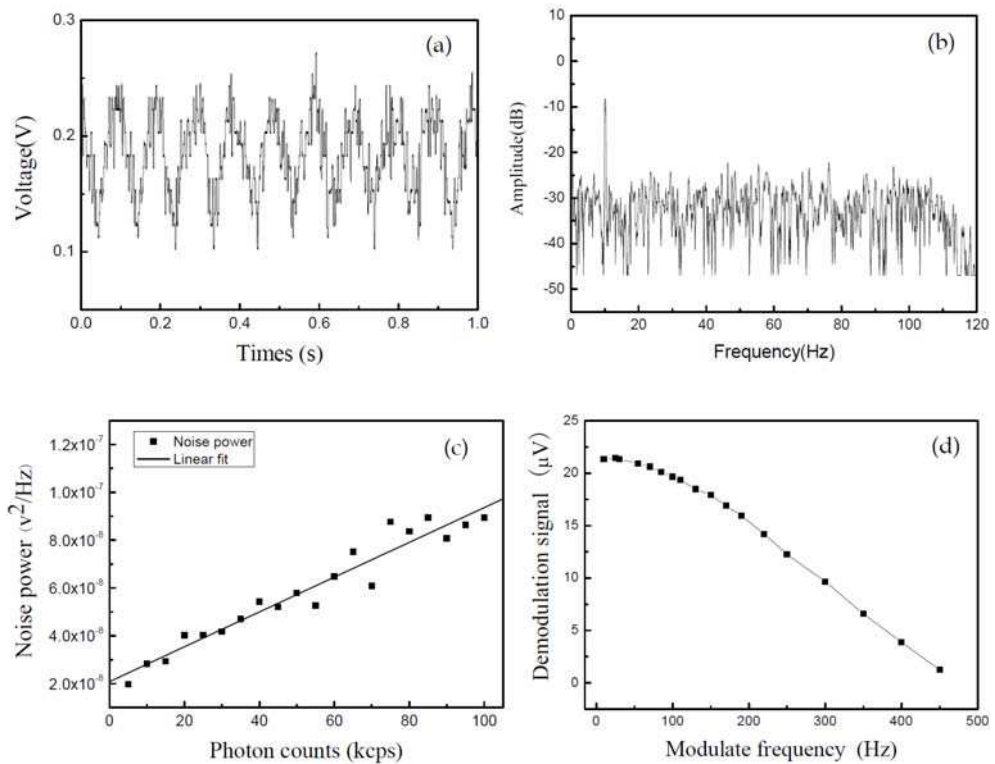
Fig. 5. The digital-to-analog signal for photon counts (a) and its noise amplitude spectral characteristics (b). (c) shows the linear relationship between noise power and the mean photon number. (d) is the demodulation output from the lock-in amplifier vs. modulation frequency.

magnitude higher than the corresponding noise amplitude. There is a sudden decrease at 110 kHz only because of the 110 kHz wideband of the lock-in amplifier. Fig. 5 (c) shows the linear relationship between noise power and the mean photon number. The slope is 7.2^{-8} $V^2/Hz^{1/2}$/photon.

Nevertheless, the choice of modulation frequency also affected the measurement results. As shown in Fig. 5 (d), the output signal value of lock-in amplifier will gradually decrease as the modulation frequency increasing. If the modulation frequency is lower, the data processing will need longer time, which limits the measurement speed. Increasing the modulation frequency would increase the speed of data processing, but reduce the average photon number and then reduce the measurement sensitivity. In practical applications, we need to select appropriate modulation frequency according to the average photon number.

Fig. 6 is the measurement results of the TGSPC at one of retroreflectors. The dashed line is the time distribution characteristics of TGSPC using photon counting methods directly. The counting time τ=10ms and the step of time delay is 5ps. We found the bigger counts induce the greater fluctuation. This is determined by the quantum fluctuations $(\alpha\tau)^{1/2}$ in photon

counting. The solid line is the photon counts modulation TGSPC results measured by the lock-in amplifier where the quantum fluctuations are eliminated effectively.
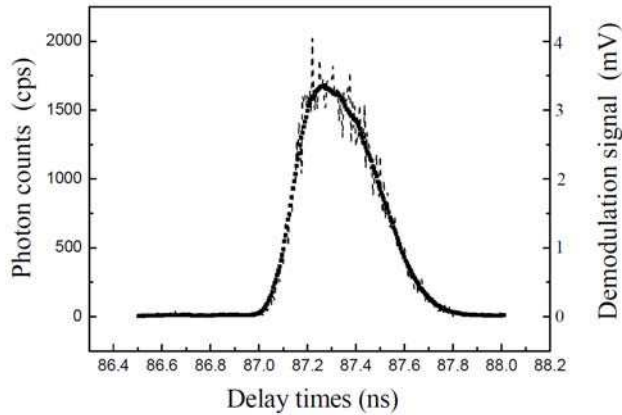

Fig. 6. TGSPC results from direct measurement of photon counting (dashed line) and photon counts modulation (dots).

Table 1 is the relationship between the slope of the low-pass filter and equivalent noise bandwidth (ENBW). Where *T* is integration time constant of lock-in amplifier. Filter slope determines the extent of the noise filter, the greater slope namely the smaller the noise equivalent bandwidth, the ability to filter out the noise being stronger. Improving SNR could be achieved by selecting the integration time of the lock-in amplifier and then changing the filter bandwidth.

Slope	*ENBW*
6dB/oct	$1/(4T)$
12dB/oct	$1/(8T)$
18dB/oct	$3/(32T)$
24dB/oct	$5/(64T)$

Table 1. The relationship between the slope of the low-pass filter and equivalent noise bandwidth *ENBW*.

The slope of the filter used in our experiments is 18 dB, integral time is *T*=100ms. The filter bandwidth of lock-in amplifier that of corresponding the noise equivalent bandwidth can be calculated *ENBW*=0.94Hz. In the place of 10 Hz modulation frequency of Fig. 5 (b), the corresponding voltage noise spectral density is $10^{-3}\,V/\sqrt{Hz}$. Then the SNR of photon counts modulated TGSPC is

$$SNR_M = 0.15V/(10^{-3}\,V/\sqrt{Hz} \times \sqrt{0.94Hz}) = 159 \ . \tag{8}$$

With the average photon number at the peak $\alpha = 1700 cps$, maximum SNR of photon counting can be obtained from equation (3)

$$SNR_{PC} = \sqrt{\alpha\tau} = 4.12 \ . \tag{9}$$

The signal-to-noise improvement ratio corresponds to the photon counting modulation is

$$SNIR = 20\log(SNR_M/SNR_{PC}) = 20\log(159/4.12) = 31.7dB\,. \tag{10}$$

3.3 Single photon lock-in and optimal threshold for the discriminator

We have shown that the photon counts lock-in can improve the SNR of TGSPC. However, the analog conversion also makes it difficult for one to measure relative small-signal amplitude by normalizing it against the DC background. We will demonstrate experimentally the single photon lock-in and the optimal discriminate determination.

The experimental setup is shown in Fig. 3. A sine-wave function generator is triggered by the 1/40 divider from laser pulses frequency f_p, with repetition frequency f_s=100 kHz, as the modulation signal and added onto the AOM's driver. The analog output of the single photon detector is connected to the photon counter (SRS SR400). Discriminators of SR400 are provided with a selectable threshold in 0.2 mV steps. And the outputs from SR400 are 100 ns pulses. It is found that SR400 output with the discriminate voltage at 184 mV has the same photon counting value as that from the detector digital output. And the photon counting will be carried out at the 184 mV threshold.

For a sine-wave modulation, the probability for single photon being detected is

$$P = \frac{\eta}{1+d}\big(1 + d\cos(2\pi f_s + \phi)\big)\,, \tag{11}$$

where d represents the depth of modulation, ϕ is the signal phase. Here we assumed η is the maximum detection efficiency during the modulation. With the experimental parameter above, we have $d\approx1$.

The single photon lock-in method we used here means that the pulses from the SR400 output are attenuated and then directly demodulated by the lock-in amplifier. The synchronous 100 kHz sine-wave was added onto the lock-in amplifier as the reference signal.
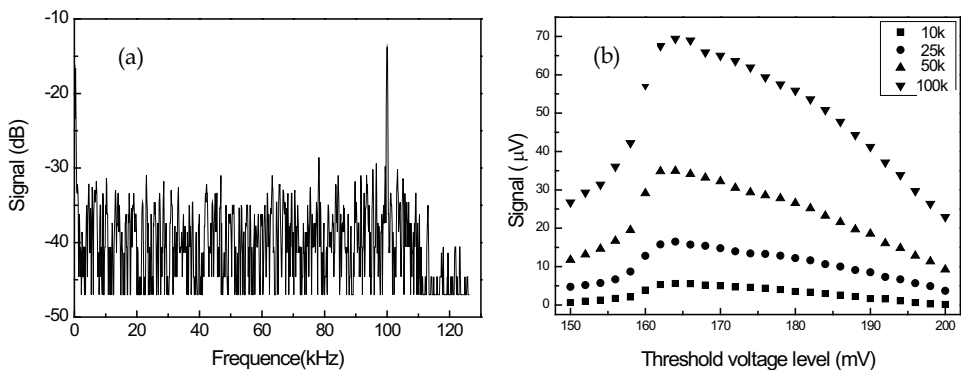

Fig. 7. (a) The frequency spectrum of single photons lock-in. (b) The single photon lock-in output corresponding to different mean photon counts, 10 kcps, 25 kcps, 50 kcps and 100 kcps, respectively.
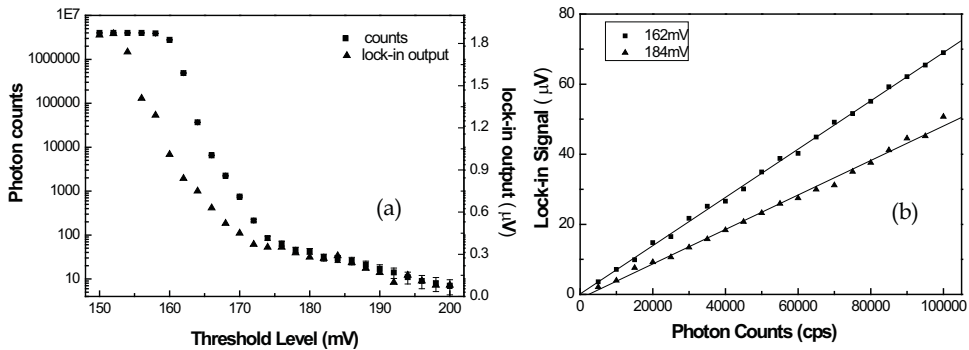
Fig. 8. (a) Dark count and its lock-in measurements vs discriminate threshold. (b) Single photon lock-in outputs vs threshold with different photon counts. The single photon lock-in outputs vs photon counts for threshold being 162 mV and 184 mV, respectively.

The frequency spectrum of the monitor out of lock-in amplifier is shown in Fig. 7 (a). Here, the mean photon number is 100 kcps and the SR400 threshold is 184mV. Note that the single photon modulation signal at the place of frequency 100 kHz. As the dark counts of the SPAD follow Poisson statistics, i.e., dominating shot noise with white noise spectral density, we found the uniform distribution of the background noise. The effect of Flicker noise (l/f) noise on the accuracy of measurements can be ignored. At lower threshold, the (l/f) noise may become dominant, so we choose the 100 kHz for single photon modulation, due to the higher noise in the low-frequency region.

As shown in Fig. 7 (b), when we change the level discrimination from 184 mV to 162 mV, it is found that the dark counts increase quickly which cover 4 orders of magnitude where the weak photon signals will be immerged in the case at lower threshold. The limit to detection efficiency is primarily device saturation from dark counts.

In Fig. 7 (b), we show the single photon lock-in output corresponding to different mean photon counts, 10 kcps, 25 kcps, 50 kcps and 100 kcps, respectively. The data are obtained by first setting the discriminate voltage, and measuring the mean photon counts and lock-in output respectively. The traces show the discriminate threshold can be optimized at 162 mV where the lock-in has the maximum output.

Accordingly, we have measured the lock-in output with the lock-in integrated time 100 ms, and the equivalent noise bandwidth for bandpass filter Δf =1 Hz. It is interesting to note that the lock-in output increase only 4 times from 184 mV to 162 mV in Fig. 8 (a).

The demodulated signals versus photon counts for discriminate threshold being 162 mV and 184 mV are shown in Fig. 8 (b). The two curves show that the intensity of single photon lock-in signals are increasing linearly as the photon counts increased. The slope for the fitted line is 1.24 μV/kcps at 184 mV threshold, and 2.32 μV/kcps at 162 mV, respectively. It is shown that the detected efficiency with single photon lock-in at 162 mV is 1.87 times bigger than that of the photon counting method at 184 mV.

We have demonstrated our measurement system in TGSPC experiment for a 3m-length displacement between the two retroreflectors. The backscattered photons reach to the InGaAs single photon detectors through a fiber optical circulator, as shown in Fig. 9. With the 162 mV optimal threshold, the single photon lock-in for TGSPC experiment is shown as Fig. 9, where the backscattered signal is presented as a function of length. Here it is found

that the dark count and the photon shot noise are restrained, and clearly the conventional photon counting is dogged by a high dark count rate at this low threshold.
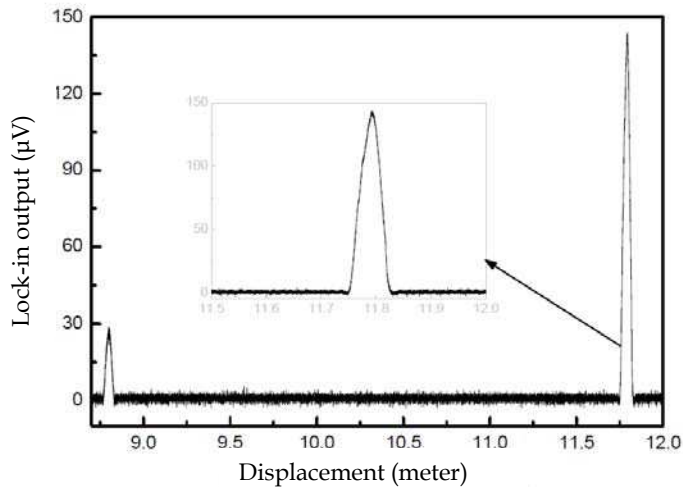

Fig. 9. The TGSPC measurement by using single photons lock-in with the optimal threshold 162 mV.

4. Conclusion and outlook

The single photon detection for TGSPC which has some features of broad dynamic range, fast response time and high spatial resolution, remove the effect of the response relaxation properties of other photoelectric device. We present a photon counting lock-in method to improve the SNR of TGSPC. It is shown that photon counts lock-in technology can eliminate the effect of quantum fluctuation and improve the SNR. In addition, we demonstrate experimentally to provide high detection efficiency for the SPAD by using the single photon lock-in and the optimal discriminate determination. It is shown that the background noise could be obviously depressed compared to that of the conventional single photon counting. The novel method of photon-counting lock-in reduces illumination noise, detector dark count noise, can suppress background, and importantly, enhance the detection efficiency of single-photon detector.

The conclusions drawn give further encouragement to the possibility of using such ultra sensitive detection system in very weak light measurement occasions (Alfonso & Ockman, 1968; Carlsson & Liljeborg, 1998). This high SNR measurement for TGSPC could improve the dynamic range and time resolution effectively, and have the possibility of being applied to single-photon sensing, quantum imaging and time of flight.

5. Acknowledgments

6. References

Alfonso, R. R. & Ockman, N. (1968). Methods for Detecting Weak Light Signals. *J. Opt. Soc. Am.*, Vol. 58, No. 1, (January 1968) page numbers (90-95), ISSN: 0030-3941

Arecchi, F. T.; Gatti, E. & Sona, A. (1966). Measurement of Low Light Intensities by Synchronous Single Photon Counting. *Rev. Sci. Instrum.*, Vol. 37, No. 7, (July 1966) page numbers (942-948), ISSN: 0034-6748

Becker, W. (2005). *Advanced Time-Correlated Single Photon Counting Techniques,* Springer, ISBN-10 3-540-26047-1, Germany

Benaron, D. A. & Stevenson, D. K. (1993). Optical Time-of-flight and Absorbance Imaging of Biologic Media. *Science,* Vol. 259, No. 5100, (March 1993) page numbers (1463-1466), ISSN: 0036-8075

Braun, D. & Libchaber, A. (2002). Computer-based Photon-counting Lock-in for Phase Detection at the Shot-noise Limit. *Opt. Lett.*, Vol. 27, No. 16, (August 2002) page numbers (1418-1420), ISSN: 0146-9592

Carmer, D. C. & Peterson, L. M. (1996). Laser Radar in Robotics. *Proceedings of the IEEE*, Vol. 84, No. 2, (February 1996) page numbers (299-320), ISSN: 0018-9219

Dixon, A. R.; Yuan, Z. L.; Dynes, J. F.; Sharpe, A. W. & Shields, A. J. (2008). Gigahertz Decoy Quantum Key Distribution with 1 Mbit/s Secure Key Rate. *Opt. Express,* Vol. 16, No. 23, (October 2008) page numbers (18790-18970), ISSN: 1094-4087

Dixon, G. J. (1997). Time-resolved Spectroscopy Defines Biological Molecules. *Laser Focus World*, Vol. 33, No. 10, (October 1997) page numbers (115-122), ISSN: 1043-8092

Forrester, P. A. & Hulme J. A. (1981). Laser Rangefiders. *Opt. Quant. Electron.*, Vol. 13, No. 4, (April 1981) page numbers (259-293), ISSN: 0306-8919

Gisin, N.; Ribordy, G.; Tittel, W. & Zbinden, H. (2002). Quantum Cryptography. *Rev. Mod. Phys.,* Vol. 74, No. 1, (January 2002) page numbers (145–195), ISSN: 0034-6861

Hadfield, R. H. (2009). Single-photon Detectors for Optical Quantum Information Applications. *Nat. Photonics,* Vol. 3, No. 12, (December 2009) page numbers (696-705), ISSN: 1749-4885

Hadfield, R. H.; Habif, J. L.; Schlafer, J.; Schwall, R. E. & Nam, S. W. (2006). Quantum Key Distribution at 1550 nm with Twin Superconducting Single-photon Detector. *Appl. Phys. Lett.*, Vol. 89, No. 24, (December 2006) page numbers (241129-1~3), ISSN: 0003-6951

Hiskett, P. A.; Buller, G. S.; Loudon, A. Y.; Smith, J. M.; Gontijo, I.; Walker, A. C.; Townsend, P. D. & Robertson, M. J. (2000). Performance and Design of InGaAs–InP Photodiodes for Single-photon Counting at 1.55μm. *Appl. Opt.*, Vol. 39, No. 36, (December 2000) page numbers (6818–6829), ISSN: 0003-6935

Hiskett, P. A.; Smith, J. M.; Buller, G. S. & Townsend, P. D. (2001). Low-noise Single-photon Detection at a Wavelength of 1.55 μm. *Electron. Lett.*, Vol. 37, No.17, (August 2001) page numbers (1081–1083), ISSN: 0013-5194

Huang, T.; Dong, S. L.; Guo, X. J.; Xiao, L. T. & Jia, S. T. (2006). Signal-to-noise Ratio Improvement of Photon Counting using Wavelength Modulation Spectroscopy. *Appl. Phys. Lett.,* Vol. 89, No. 6, (August 2006) page numbers (061102-1~3), ISSN: 0003-6951

Lacaita, A. L.; Francese, P. A. & Cova, S. (1993). Single-photon Optical-time Domain Reflectometer at 1.3 μm with 5 cm Resolution and High Sensitivity. *Opt. Lett.*, Vol. 18, No. 13, (July 1993) page numbers (1110–1112), ISSN: 0146-9592

Lacaita, A.; Zappa, F.; Cova, S. & Lovati, P. (1996). Single-photon Detection Beyond 1 μm: Performance of Commercially Available InGaAsInP Detectors. *Appl. Opt.*, Vol. 35, No. 16, (June 1996) page numbers (2986–2996), ISSN: 0003-6935

Lee D.; Yoon, H. & Park, N. (2006). Optimization of SNR Improvement in the Noncoherent OTDR Based on Simplex Codes. *J. Lightwave Technol.,* Vol. 24, No. 1, (January 2006) page numbers (322-328), ISSN: 0733-8724

Legre, M.; Thew, R.; Zbinden, H. & Gisin, N. (2007). High Resolution Optical Time Domain Reflectometer Based on 1.55μm Up-conversion Photon-counting Module. *Opt.Express,* Vol. 15, No. 13, (June 2007) page numbers (8237 -8242), ISSN: 1094-4087

Leskovar, B. & Lo, C.C. (1976). Photon Counting System for Subnanosecond Fluorescence Lifetime Measurements, *Rev. Sci. Instrum.,* Vol. 47, No. 9, (September 1976) page numbers (1113 – 1121), ISSN: 0034-6748

Mäkynen, A. J.; Kostamovaara, J. T. & Myllylä, R. A. (1994). Tracking Laser Radar for 3-D Shape Measurements of Large Industrial Objects Based on Time-of-Flight Laser Rangefinding and Position-Sensitive Detection Techniques. *IEEE T. Instrum. Meas.*, Vol. 43, No. 1, (February 1994) page numbers (40-49), ISSN: 0018-9456

Moring, I.; Heikkinen, T.; Myllylä, R. & Kilpelä, A. (1989). Acquisition of Three Dimensional Image Data by a Scanning Laser Range Finder. *Opt. Eng.*, Vol. 28, No. 8, (August 1989) page numbers (897 – 902), ISSN: 0091-3286

Murphy, M. K.; Clyburn, S. A. & Veillon, C. (1973). Comparison of Lock-in Amplification and Photon Counting with Low Background Flames and Graphite Atomizers in Atomic Fluorescence Spectrometry. *Anal.Chem.,* Vol. 45, No. 8, (July 1973) page numbers (1468-1473), ISSN: 0003-2700

Namekata, N.; Sasamori, S. & Inoue, S. (2006). 800 MHz Single-photon Detection at 1550-nm using an InGaAs/InP Avalanche Photodiode Operated with a Sine Wave Gating. *Opt. Express,* Vol. 14, No. 21, (September 2006) page numbers (10043–10049), ISSN: 1094-4087

Pellegrini, S.; Buller, G. S.; Smith, J. M.; Wallace, A. M. & Cova, S. (2000). Laser-based Distance Measurement using Picosecond Resolution Time-correlated Single-photon Counting. *Meas. Sci. Technol.*, Vol. 11, No. 6, (June 2000) page numbers (712–716), ISSN: 0957-0233

Pellegrini, S.; Warburton, R. E.; Tan, L. J. J.; Jo Shien Ng; Krysa, A. B.; Groom, K.; David, J. P. R.; Cova, S.; Robertson, M. J. & Buller, G. S. (2006). Design and Performance of an InGaAs-InP Single-photon Avalanche Diode Detector. *IEEE J. Quant. Elect.*, Vol. 42, No. 4, (April 2006) page numbers (397–403), ISSN: 0018-9197

Poultney, S. K. (1972). Single-photon Detection and Timing: Experiments and Techniques, In: *Adv. Electron. El. Phys.*, L. Marton and Claire Marton (Ed.), Vol. 31, page numbers (39–117), Elsevier, ISBN: 9780120145317, Netherlands

Poultney, S. K. (1977). Single Photon Detection and Timing in the Lunar Laser Rranging Experiment. *IEEE T. Nucl. Sci.*, Vol. 19, No. 3, (June 1972) page numbers (12-17), ISSN: 0018-9499

Princeton Light Wave, (2006).
    http://princetonlightwave.com/content/PGA-600%20V1.01.pdf.

Ribordy, G.; Gautier, J. D.; Zbinden, H. & Gisin, N. (1998). Performance of InGaAs/InP Avalanche Photodiodes as Gated-mode Photon Counters. *Appl. Opt.* Vol. 37, No. 12, (January 1998) page numbers (2272–2277), ISSN: 0003-6935

Ribordy G.; Gisin, N.; Guinnard, O.; Stucki, D.; Wegmuller, M. & Zbinden, H. (2004). Photon Counting at Telecom Wavelengths with Commercial In-GaAs/InP Avalanche Photodiodes: Current Performance. *J. Mod. Opt.*, Vol. 51, No. 9, (May 2004) page numbers (1381–1398), ISSN: 0950-0340

Roussev, R. V.; Langrock, C.; Kurz, J. R. & Fejer, M. M. (2004). Periodically Poled Lithium Niobate Waveguide Sum-frequency Generator for Efficient Single-photon Detection at Communication Wavelengths. *Opt. Lett.* Vol. 29, No. 13, (July 2004) page numbers (1518-1520), ISSN: 0146-9592

Stanford Research Systems, (1995). "Signal recovery with photomultiplier tubes," Application Note 4,
    http://www.srsys.com.

Stanford Research Systems, (1999). "DSP Lock-in Amplifier SR850," Chap. 3,
    http://www.srsys.com.

Stucki, D.; Ribordy, G.; Stefanov, A.; Zbinden, H.; Rarity, J. G. & Wall, T. (2001). Photon Counting for Quantum Key Distribution with Peltier Cooled InGaAs–InP APDs. *J. Mod. Opt.*, Vol. 48, No. 13, (November 2001) page numbers (1967–1981), ISSN: 0950-0340

Takesue, H.; Diamanti, E.; Langrock, C.; Fejer, M. M. & Yamamoto, Y. (2006). 1.5 μm Photon-counting Optical Time Domain Reflectometry with a Single-photon Detector based on Upconversion in a Periodically Poled Lithium Niobate Waveguide. *Opt. Lett.*, Vol. 31, No. 6, (March 2006) page numbers (727–729), ISSN: 0146-9592

Thew, R. T.; Stucki, D.; Gautier, J. D.; Zbinden, H. & Rochas, A. (2007). Free-running InGaAs/InP Avalanche Photodiode with Active Quenching for Single Photon Counting at Telecom Wavelengths. *Appl. Phys. Lett.,* Vol. 91, No. 20, (November 2007) page numbers (201114-1~3) ISSN: 0003-6951

Tilleman, M. M. & Krishnaswami, K. K. (1996). Design of Fibre Optic Relayed Laser Radar. *Opt. Eng.,* Vol. 35, No. 11, (May 1996) page numbers (3279-3284), ISSN: 0091 3286

Warburton, R. E.; Itzler, M. & Buller, G. S. (2009). Free-running Room Temperature Operation of an InGaAs/InP Single-photon Avalanche Diode. *Appl. Phys. Lett.*, Vol. 94, No. 7, (February 2009) page numbers (071116-1~3), ISSN: 0003-6951

Wegmüller, M.; Scholder, F. & Gisin, N. (2004). Photon-counting OTDR for Local Birefringence and Fault Analysis in the Metro Environment. *J. Lightwave Technol.,* Vol. 22, No. 2, (February 2004) page numbers (390-400), ISSN: 0733-8724

Yano, H.; Aga, K.; Kamei, H.; Sasaki, G. & Hayashi, H. (1990). Low-Noise Current Optoelectronic Integrated Receiver with Internal Equalizer for Gigabit-per-Second Long-Wavelength Optical Communications. *J. Lightwave Technol.,* Vol. 8, No.9, (September 1990) page numbers (1328-1333), ISSN: 0733-8724

Yoshizawa, A.; Kaji, R. & Tsuchida, H. (2004). Gated-mode Single-photon Detection at 1550 nm by Discharge Pulse Counting. *Appl. Phys. Lett.,* Vol. 84, No. 18, (April 2004) page numbers (3606–3608), ISSN: 0003-6951

Laser Pulse Phenomena and Applications

Edited by Dr. F. J. Duarte

Pulsed lasers are available in the gas, liquid, and the solid state. These lasers are also enormously versatile in their output characteristics yielding emission from very large energy pulses to very high peak-power pulses. Pulsed lasers are equally versatile in their spectral characteristics. This volume includes an impressive array of current research on pulsed laser phenomena and applications. *Laser Pulse Phenomena and Applications* covers a wide range of topics from laser powered orbital launchers, and laser rocket engines, to laser-matter interactions, detector and sensor laser technology, laser ablation, and biological applications.

How to reference

In order to correctly reference this scholarly work, feel free to copy and paste the following:

Liantuan Xiao, Xiaobo Wang, Guofeng Zhang and Suotang Jia (2010). Time-gated Single Photon Counting Lock-in Detection at 1550 nm Wavelength, Laser Pulse Phenomena and Applications, Dr. F. J. Duarte (Ed.), ISBN: 978-953-307-405-4, InTech, Available from: http://www.intechopen.com/books/laser-pulse-phenomena-and-applications/time-gated-single-photon-counting-lock-in-detection-at-1550-nm-wavelength

INTECH
open science | open minds